Sopok
ct

AIAA-2000-3650
Cannon Coating Erosion Model With Updated M829E3 Example

S. Sopok
US Army Benet Labs
Watervliet, NY

DISTRIBUTION STATEMENT A
Approved for Public Release
Distribution Unlimited

20040218 192

36th AIAA/ASME/SAE/ASEE Joint Propulsion Conference & Exhibit
16-19 July 2000
Huntsville, Alabama

For permission to copy or to republish, contact the American Institute of Aeronautics and Astronautics, 1801 Alexander Bell Drive, Suite 500, Reston, VA, 20191-4344.

AIAA-2000-3650

(36th AIAA Joint Propulsion Conference, Huntsville AL, 16-19 July 2000)

CANNON COATING EROSION MODEL WITH UPDATED M829E3 EXAMPLE

Sam Sopok
US Army Benet Labs, Watervliet NY

ABSTRACT

The cannon coating erosion model is necessary since most current/future cannons will require a refractory metal bore coating. Coated cannon bore erosion does not simply proceed in a outward to inward ablative fashion due to coating spalling. Typical firing induced cannon erosion sequentially includes heat check cracking of the refractory metal coating, coating shrinkage leading to progressive widening of these cracks, combustion gas induced interface degradation of the exposed substrate metal, interfacial spalling of refractory metal coating platelets due to linked interfacial degradation which forms pits, and subsequent substrate metal gas wash to erosion condemnation. The purpose of this paper is to review typical cannon erosion mechanisms, highlight the resultant cannon coating erosion model, show how this very critical coatings model incorporates into our overall cannon erosion code (CEC), and provide an example. This example is an updated erosion prediction for the experimental non-ablative M829E3 kinetic energy tank round which puts the program just shy of its 180 round target. In addition, this example is for both HEAT type rounds which alter the M829E3 erosion pattern and the absence of these HEAT type rounds. This cannon coating erosion model correlates very well with laboratory/firing data and has been used for three years on a number of important Army and Navy gun systems.

INTRODUCTION

At the 31st AIAA Joint Propulsion Conference, our erosion team introduced investigative results of typical cannon erosion mechanisms and our associated unified computer model for predicting thermal-chemical-mechanical erosion in cannons.[1] Periodically published updates have followed as new cannon erosion investigations are conducted leading to the associated evolution of this erosion model. These computational erosion predictions are guided and calibrated by substantial data from gun system firings and laboratory analysis of fired specimens. This cannon erosion code was derived and refined from a set of enormously successful ballistic missile and space program reentry vehicle nose-tip, heat shield and nozzle codes. This original cannon code, like its rocket counterpart, ablated the outer-most surface material exposed to the combustion gases and then proceeded inward to ablate additional subsurface materials in a successive fashion. Based on these cannon erosion mechanisms, this original cannon erosion model is still used successfully today to predict erosion of non-coated steel cannon bores. For coated cannon bores, this original cannon erosion model was used only two years, could only make order-of-magnitude predictions or qualitative comparisons, and required significant improvement. An improved cannon coating erosion model based on typical refractory metal coated cannon bore erosion mechanisms[1-2] is given in this paper along with the mentioned experimental gun system example.

COMPUTATIONAL AND EXPERIMENTAL METHODS

Our Cannon Erosion Code (CEC) consists of a number of interactively linked codes and is used to predict wall temperature profiles and thermal-chemical-mechanical erosion profiles in cannons.[1-2] This overall

"Approved for public release, distribution unlimited".
This is declared a work of the U.S. Government and not subjected to copyright protection in the United States.

erosion code includes the CCET thermo-chemistry cannon code,[1-3] XNOVAKTC interior ballistics code,[1,2,4] MABL boundary layer cannon code,[1,2,5] and the MACE thermal & erosion cannon code.[1,2,6] These erosion predictions are guided and calibrated by substantial gun system firing data and fired specimen analyses.

RESULTS AND DISCUSSION

The experimental non-ablative M829E3 kinetic energy (KE) tank round example with and without significant HEAT type rounds is used to show the step-by-step process of how the coating cannon erosion model is incorporated into the overall cannon erosion code.

The CCET thermochemistry cannon code uses initial chemical/materials input to calculate gas and thermochemistry data for the interior ballistics, boundary layer, and thermal & erosion codes. The example M829E3/RPD380 propellant consists of approximately 59% nitrocellulose, 25% nitroglycerine, 15% diethylene glycol dinitrate and 1% other minor species. Its igniter consists of 25 grams black powder and 25 grams CBI. Actual measured thermochemical data are used to calibrate the calculation for gas products.

The XNOVAKTC interior ballistics code uses thermochemistry code output and gun system defining inputs to calculate the time-dependent core flow data for the boundary layer code. The example gun system includes the 17.3 foot 120mm M256 cannon, its experimental non-ablative 18 pound RPD380 propellant, and projectile details that are classified. Actual measured pressure gauge and radar data are used to calibrate this time-dependent core flow calculation.

Figures 1-2 show the experimental non-ablative M829E3 round XNOVAKTC interior ballistic results for respective maximum values of gas pressure (Pg) and gas temperature (Tg) as a function of selected axial positions at selected round conditioning temperatures. Maximum values were used instead of time dependent data to simplify the appearance of these figures. Both decrease with increasing axial position. Gas velocity is omitted due to its classified nature. Selected axial positions include 0.6, 1.6, 2.2, 3.3, and 5.1 meters from the rear face of the tube (RFT) while the selected round conditioning includes the hot (49 C), ambient (21 C), and cold (-31 C) temperatures. These five selected axial positions and three selected round conditioning temperatures are used exclusively throughout the rest this paper. The significance of the 0.6 meter position is that it is slightly past the origin of the bore and it is the mean peak eroded position when both M829E3 and HEAT type rounds are mixed. The significance of the 1.6 meter position is that it is the mean peak eroded position when M829E3 rounds are fired without HEAT type rounds. The significance of the 2.2 meter position is that it is the mean peak eroded position when M829A2 rounds are fired without HEAT type rounds. The significance of the 3.3 meter position is that it is near the bore evacuator holes. The significance of the 5.1 meter position is that it is near the muzzle. Distributions and associated standard deviations exists around these various mean eroded positions.

The MABL boundary layer cannon code uses thermochemistry and interior ballistics code outputs to calculate boundary layer characteristics for the thermal & erosion code. Figures 3-4 show the experimental non-ablative M829E3 round MABL boundary layer results for respective maximum values of recovery enthalpy (Hr) and cold wall heat flux (Qcw) as a function of selected axial positions at selected round conditioning temperatures. Maximum values were again used instead of time dependent data to simplify the appearance of these figures. Both increase with increasing axial position to a 1.6 meter RFT peak and decrease thereafter to the muzzle. The 0.6 meter RFT mean peak heat transfer bore position calculated by the interior ballistic analysis is shifted to a 1.6 meter RFT mean peak bore position calculated by the boundary layer analysis due to the 1600 K combustion case gas cooling effects and turbulent gas mixing/heating effects.

The CCET thermochemistry cannon code uses initial chemical/materials input to calculate gas-wall thermochemistry data for the thermal & erosion code. Actual measured thermochemical data are used to calibrate the calculation for gas-wall products and gas-wall

reaction rates. Figure 5 shows the experimental non-ablative M829E3 round CCET thermo-chemical results for mean values of reacting gas-wall enthalpy (Hgw) and ablation potential (Ba) as a function of wall temperatures (Twall) for the HC chromium plate-gun steel substrate wall materials. Mean values were used to simplify the appearance of this figure.

The MACE thermal & erosion cannon code uses thermochemistry code output, boundary layer code output, material properties input, round type input and firing scenario input to calculate wall temperature profiles and wall erosion profiles as a function of axial position, radial position, time, round conditioning temperature, number of rounds, and type of rounds. Actual measured gas-wall kinetic rate function data, thermocouple data, microscopic coating/steel crack & pit data, and reaction/ diffusion/phase change degradation data are used to calibrate this wall thermal and erosion calculation. The measurement and use of these four types of data are explained in the remainder of the paper.

Measured gas-wall kinetic rate function data are used to calibrate the thermochemical calculation and transform this chemical equilibrium calculation into a partial chemical kinetic calculation. Chemical analysis of crack & pit wall layers, interface wall layers, bore surface layers, subsurface void residues, and surface residues further guided gas-wall kinetics calibration. Thermocouple data are used to calibrate the wall thermal profile calculation.

Figure 6 shows typical gun steel substrate exposure for cannons with a mixture of experimental non-ablative M829E3 rounds and other KE rounds. This data is from a small sampling of HC chromium plated M256 cannons which quantifies cracking, pitting and chromium plate loss. These cannons were condemned on erosion and had numerous condemning scoring holes centered at the 1.6 meter RFT position. This substrate exposure is a function of the selected axial positions at 1% (nondestructively measured at post-proofing), 50% (exponentially estimated), 80% (exponentially estimated), and 100% (nondestructively and destructively measured at erosion condemnation) of equivalent ambient conditioned M829E3 erosion life based on previous work.[2]

These nondestructive substrate exposure measurements are made by a magnifying bore scope with a calibrated scale while the corresponding destructive measurements are made by metallographic, SEM-EDS, and ESCA techniques. These nondestructive measurements are based on the verified assumption that substrate exposure is approximately equal at the surface and interface. Bore position dependent and equivalent erosion life dependent substrate exposure measurements include average axial and circumferential crack/pit frequency, average axial and circumferential crack/pit width, and average axial and circumferential platelet width. An improved comprehensive measurement procedure is often used that includes crack/pit frequency, crack/pit width, and platelet width distributions instead of this simple averaging. These measured data are used as a substitute for a thermal-mechanical crack and pit model that is yet to be developed. This measured substrate exposure pattern correlates with the boundary layer heat transfer pattern where both increase with increasing axial position to a 1.6 meter RFT peak and decrease thereafter to the muzzle.

Figure 7 (2000X) and Figure 8 (1000X) are micrographic examples of destructive substrate exposure measurements made by a SEM-EDS technique but metallographic, EPMA, and ESCA techniques also gave similar micrographic results. For the M829E3 1.6 meter RFT peak eroded position, these figures respectively illustrate very typical enabling and accelerating erosion mechanism steps. Figure 7 shows a very fine HC chromium plate crack that provides a narrow combustion gas path to the gun steel producing limited interfacial gun steel degradation. In contrast, Figure 8 shows a progressively widened/extended HC chromium plate crack due to chromium shrinkage that provides a wide combustion gas path to the gun steel producing substantial interfacial gun steel degradation. If this cannon were still in service, linked interfacial degradation of the main crack to the adjacent fine crack in Figure 8 would lead to eventual spalling of the associated chromium platelet. Using the above techniques coupled with their associated chemical analysis techniques, these and similar micrographs illustrate phase change degradation (diffusion induced carburized white layer and heat

affected zone on/into exposed gun steel, chromium recrystallization) and chemical reaction degradation (oxidation and sulfidation of exposed gun steel forming semi-metallic layers) of the gun steel substrate under the 130 um thick chromium plate and particularly at crack and interfacial walls/wall layers.

Two other factors that enhance chromium plate-gun steel substrate interfacial degradation of its metals and interstitials are the increased reactivity of the interface due to its higher energy state and interfacial porosity due to firing induced local diffusion.[1] For refractory metal coated steels, a group from LSU has found that surface refractory metal coating oxides seed heat checking cracks, high temperature combustion oxidizes steel crack walls and interfaces forming brittle products with inferior mechanical properties, and atomic hydrogen hops between crack wall oxides to migrate to its lowest free energy at a crack tip.[7]

HC chromium plate has a passivating oxidation temperature at about 2000 K, a sulfidation temperature above 2130 K and a melting point at about 2130 K. Gun steel has an expansive flaking iron oxidation temperature at about 1050 K, a iron sulfidation temperature at about 1270 K, an iron oxide melting point at about 1640 K, an iron sulfide melting point at about 1470 K, and a gun steel melting point at about 1720 K.

Figures 9-11 show the experimental non-ablative M829E3 MACE maximum wall temperature (Twall) results for the HC chromium surface, gun steel interface, and gun steel surface minus 0.13 mm as a function of the selected axial positions at the selected round conditioning temperatures. For these figures, maximum values were also used instead of time dependent data to simplify their appearance. The overall maximum wall temperature for the HC chromium surface is about 1700 K which explains its inertness, for the gun steel interface is about 1270 K which explains its reactivity, and for the gun steel surface minus 0.13 mm is about 1440 K which explains its reactivity. For these three figures, the calculated maximum wall temperature patterns correlate with the boundary layer heat transfer pattern where both increase with increasing axial position to a 1.6 meter RFT peak and decrease thereafter to the muzzle.

Now that the typical erosion mechanisms for coated cannons have been reviewed, it will now be shown how these mechanisms are modeled and incorporated into our overall cannon erosion code. Core flow gases at the combustion gas temperature collide with the bore surface and convectively transfer a portion of their energy to the wall. This convective bore surface heating is related to the bore surface temperature.

When a bore coating platelet spalls forming a pit that is at least 33% wider than the coating depth then a portion of the core flow combustion gases collide with the exposed substrate interface and convectively transfer a portion of their energy to this interface at a rate approximately equal to that of the bore surface. This convective substrate interface heating is related to that interface temperature and approximately equal to the bore surface temperature. This wide pit-maximum convective heating of the substrate interface is designated case one. HC chromium coating thickness is typically 0.005" generating a required pit width of at least 0.0067" for the experimental M829E3 round.

When a bore coating platelet spalls forming a pit that is progressively narrower than case one's pit width then a portion of the core flow combustion gases collide with the exposed substrate interface and convectively transfer a portion of their energy to this interface at a rate that is progressively less than that of the bore surface due to the increase of energy reducing collisions. This progressively decreasing convective substrate interface heating is related to that interface temperature and progressively less than the bore surface temperature. As the crack/pit width progressively narrows, the mean free path of the gas molecules decreases due to energy reducing collisions that reduce the initial convective heat transfer rate to a value that is progressively closer to that of the unexposed conductive heat transfer rate of the interface. This transition from wide to infinitesimally small crack/pit-transition from maximum to infinitesimally small convective heating of the substrate interface is designated case two.

When a bore coating has a very fine crack forming a infinitesimally narrow pit then the core flow combustion gases never reach the substrate interface without many energy reducing collisions that reduce the initial convective heat transfer rate to that of the unexposed conductive heat transfer rate of the interface. This infinitesimally small convective substrate interface heating is related to that interface temperature and approximately equal to the unexposed substrate interface temperature. This infinitesimally small crack/pit-infinitesimally small convective heating of the substrate interface is designated case three. Very fine HC chromium crack widths are typically 0.00001" for the experimental M829E3 round.

A cubic function of the form $y=a+bx^3$ uses the above convective heating case one and conductive heating case three extremes for calibration to predict a resultant substrate interface temperature for a given crack width as follows:

$$Tiy = Tiu + [((Ts - Tiu) / Wc^3) (Wx^3)] \qquad (1)$$

where Tiy is the resultant substrate interface temperature for a given crack/pit width, Tiu is the unexposed substrate interface temperature which is approximately equal to the substrate interface temperature of an infinitesimally small crack/pit width from Figure 10, Ts is the bore surface temperature which is approximately equal to the fully convective substrate interface temperature with a crack/pit width that is at least 33% greater than the coating thickness from Figure 9, Wc is the fully convective crack/pit width that is at least 33% greater than the coating thickness from micrographs similar to Figures 7-8, and Wx is a given crack/pit width from substrate exposure data that generated Figure 6. The first term on the right is the y-intercept which is the substrate interface temperature due to conductive heating. The second term on the right in brackets is the associated temperature correction for convective heating that ranges from infinitesimally small to the difference between Ts – Tiu. The Tiy value changes slowly at first with increasing Wx and then more rapidly as it approaches Wc due to the cubic function. For similar cracks/pits, Tiy in this equation varies significantly with axial position and rounds to erosion condemnation. For a gun system that has not been built or fired, crack/pit data can possibly be approximated from a similar gun system. Using this equation, Figure 12 shows the calibrating extreme measured points and the calculated interior points for the non-ablative M829E3 maximum exposed interface temperature as a function of HC chromium crack/pit width at selected axial positions.

This equation correlates and has been successfully applied to numerous advanced medium and large caliber gun systems over the last three years based on measured firing related data from their most extreme rounds. The measurements include phase change degradation data (diffusion induced carburized white layer and heat affected zone on/into exposed gun steel, chromium recrystallization) and chemical reaction degradation data (oxidation and sulfidation of exposed gun steel forming semi-metallic layers). The existence and depth of these measured degradations into the exposed gun steel substrate depends on and correlates with the magnitude of the related positional dependent wall temperature profiles. These measurements were particularly focused on the exposed gun steel substrate at the crack/pit/interface walls and wall layers.

After the resultant substrate interface temperatures are calculated for the position and round dependent crack/pit widths then the heat transfer multipliers in the MACE code are adjusted on a trial and error basis to achieve these resultant substrate interface temperatures and their corresponding substrate interface ablation rates. The adjustment of these heat transfer multipliers, raises the associated Tiu values to the resultant Tiy values. In addition, as the measurable interface degradation progresses, the interface contact variable in the MACE code is also adjusted as a function of axial position and rounds to erosion condemnation. The transition from case one through case two to case three is computed for the life of each crack/pit from its onset to erosion condemnation based on substrate exposure data as a function of position and rounds fired.

Interface and gun steel substrate degradation in a crack or pit is computed by the area under a temperature-time curve above a

degradation threshold such as the ~1050 K oxidation of iron by oxygen, the ~1270 K oxidation of iron by sulfur, the ~1470 K melting of this iron-sulfur compound, the ~1640 K melting of this iron-oxygen compound, and the ~1720 K melting of gun steel. Position and round dependent interface degradation thickness' are measured at the exposed gun steel substrate interface and they are consumed by the ablation rate associated with Tiy above the ablation threshold. For a given interface degradation thickness and associated Tiy ablation rate, the ablation of the exposed gun steel interface under a chromium platelet is calculated in a linear strand burning fashion. When any type of degradation of the exposed gun steel interface thickness under this coating platelet merges from two adjacent cracks/pits then the coating platelet spalls and gas wash onset begins.

Whether trainers or advanced prototype rounds are fired, very few type-classified or experimental cannons are spared some degree of heat checking in their gun steel coating. A crack or pit of any kind in the brittle M256 HC chromium coating provides a mass transport path to the gun steel. The severity and frequency of the coating heat checking cracks/pits are exponential erosion multipliers. Increasing either exposes the gun steel substrate interface to more combustion gases. The important question to ask is how much gun steel substrate exposure. Specifically, increasing the crack or pit width results in increased interfacial temperature due to increased convective heating which rises exponentially for large widths. Furthermore, increasing the crack or pit frequency results in a decreased merging distance for interfacial substrate degradation between two adjacent cracks/pits to spall a platelet which rises exponentially for large crack or pit frequencies.

An additional exponential erosion multiplier occurs above each of the mentioned exposed interfacial gun steel-combustion gas reaction thresholds. The important question to ask here is how far above these thresholds. Specifically, the reaction rate above the combustion gas/exposed gun steel interface reaction threshold rises exponentially with increasing temperature based on the Arrhenius equation. Combustion gas chemistry, pressure, velocity, and other factors play a lesser role in increasing gas-wall reaction rates. The coating erosion model requires measurable gun steel reactivity data as a function of gas-wall pressure, temperature and velocity. When this data is not available in the literature, it is measured in-house for each gun system using specialized testers.

Using the coupled MACE and coatings model calculations, Figures 13-14 show the experimental non-ablative M829E3 round cumulative erosion results. These include the respective values of cumulative rounds to 0.13 mm erosion (gun steel gas wash onset) and 5 mm erosion (erosion condemnation) as a function of the selected axial positions at selected round conditioning temperatures. The data in these two figures both inversely correlate with the predicted M829E3 boundary layer heat transfer and substrate exposure patterns above where these erosion values decreased to a 1.6 meters RFT minimum and increased thereafter.

Figures 15 is simply a summary of Figures 13-14 at only the erosion condemnation governing 1.6 meter RFT peak eroded position. Cumulative erosion versus cumulative equivalent M829E3 rounds at 1.6 meters RFT is plotted. For the respective 49 C, 21 C, -32 C, and equal distribution cases at this position, achievement of the 0.13 mm gun steel gas wash onset depth is at about 40, 65, 60 and 55 rounds while achievement of the 5 mm erosion condemnation depth is at about 130, 210, 190 and 170 rounds. A preliminary estimate for the experimental non-ablative ambient conditioned M829E3 round erosion EFC factor is about three based on its M829A2 counterpart.[2]

Figure 16 shows typical gun steel substrate exposure for cannons with a mixture of experimental non-ablative M829E3 rounds, HEAT/HEAT trainer type rounds, and other KE type rounds. This data is from a small sampling of HC chromium plated M256 cannons which quantifies cracking, pitting and chromium plate loss. These cannons were taken out of service at approximately 50% of their erosion life with peak erosion and numerous scoring holes centered at the 0.6 meter RFT position. This substrate exposure is a function of the selected axial positions at 1% (nondestructively

measured at post-proofing), 50% (non-destructively and destructively measured at removal from service), 80% (exponentially estimated), and 100% (exponentially estimated) of equivalent ambient conditioned M829E3 erosion life based on previous work.[2]

Figure 16 dramatically differs from Figure 6 which is for cannons with a mixture of experimental non-ablative M829E3 rounds and other KE types rounds. This difference is due to the very noticeable HEAT round fin gouging of the chromed bore surface for the first 0.3 meters of bore travel past the forcing cone producing additional/higher frequency HC chromium cracking/pitting. This additional/higher frequency HC chromium cracking/pitting is not present when HEAT type rounds are absent. The maximum gouging is centered at the 0.6 meter RFT position and diminishes after 0.3 meters of travel down bore. For experimental non-ablative M829E3 rounds, since increased crack/pit frequency (decreased coating platelet width) is a exponential erosion multiplier, the presence of HEAT round gouging allows erosion to peak at the 0.6 meter RFT position instead of the normal 1.6 meter RFT peak eroded position when these HEAT type rounds are absent. These measurements were made using techniques similar to Figure 6. On cannons where M829A2, M829A1, or M829 is the most advanced KE round, measurements have shown that HEAT type rounds have similarly altered their peak eroded bore positions.

Using the coupled MACE and coatings model calculations, Figures 17 summarizes the cumulative erosion results for cannons with a mixture of experimental non-ablative M829E3 rounds, HEAT/HEAT trainer type rounds, and other KE type rounds at the peak eroded 0.6 meter RFT position as a function of cumulative equivalent M829E3 rounds at the selected round conditioning temperatures. The peak eroded 0.6 meter RFT position governs erosion condemnation for this case. For these respective 49 C, 21 C, -32 C, and equal distribution cases at this position, achievement of the 5 mm erosion condemnation depth is at about 120, 200, 180 and 160 rounds. The peak erosion summary results in this figure are similar to the M829E3 peak erosion summary at 1.6 meters RFT in Figure 15.

REFERENCES

1. S. Dunn, S. Sopok, D. Coats, P. O'Hara, G. Nickerson, and G. Pflegl, "Unified Computer Model For Predicting Thermochemical Erosion In Gun Barrels," Proceedings of 31st AIAA Propulsion Meeting, San Diego, July 1995; Also AIAA Journal of Propulsion and Power, Volume 15, Number 4, Pages 601-612.

2. S. Sopok, R. Loomis, G. Pflegl, C. Rickard, "Preliminary Erosion Analysis For The Experimental M829E3 Kinetic Energy Round", Proceedings of 36th JANNAF Combustion Meeting, NASA Kennedy Space Center FL, October 1999.

3. D. Coats, S. Dunn, S. Sopok, "A New Chemical Equilibrium Code with Compressibility Effects", Proceedings of the 33rd JANNAF Combustion Meeting, Monterey CA, October 1996.

4. P. Gough, "The XNOVAKTC Code," Paul Gough Associates, Portsmouth NH, U.S. Army BRL-CR-627, February 1990.

5. J. Levine, "Transpiration and Film Cooling Boundary Layer Computer Program (MABL) - Numerical Solution of the Turbulent Boundary Layer Equations with Equilibrium Chemistry", NASA Marshall N72-19312, June 1971.

6. S. Dunn, "Materials Ablation Conduction Erosion Program (MACE)," Software and Engineering Associates, Inc., Carson City NV, June 1989.

7. R. Kalia, "High Temperature Oxidation of Cracks in Refractory Metal Coated Steel", Proceedings of the American Chemical Society National Meeting at New Orleans, 1999; also Air Force Research Lab-Kirkland Contractor Report by Department of Physics Concurrent Computing Laboratory for Materials Simulations (CCLMS) at Louisiana State University-Baton Rouge, 1999.

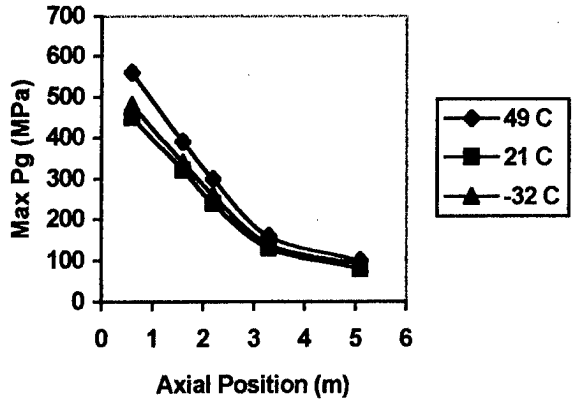

Figure 1- M829E3 NOVA Gas Pressure.

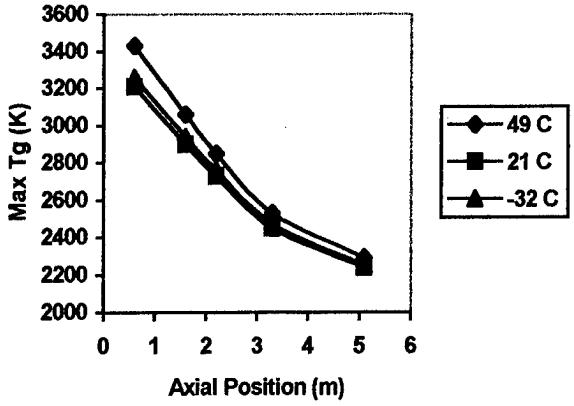

Figure 2 - M829E3 NOVA Gas Temperature.

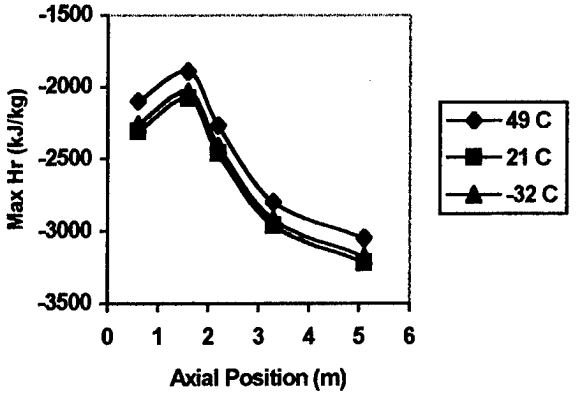

Figure 3 - M829E3 MABL Recovery Enthalpy.

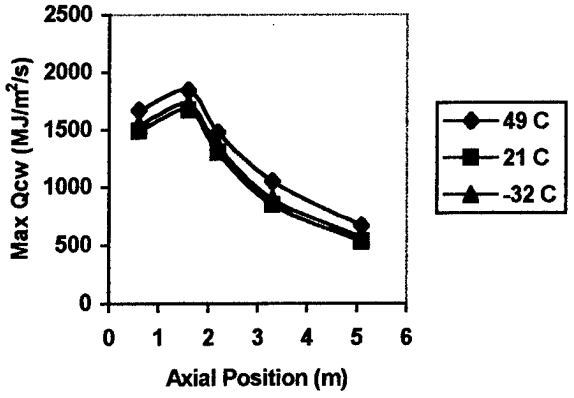

Figure 4 - M829E3 MABL Cold Wall Heat Flux.

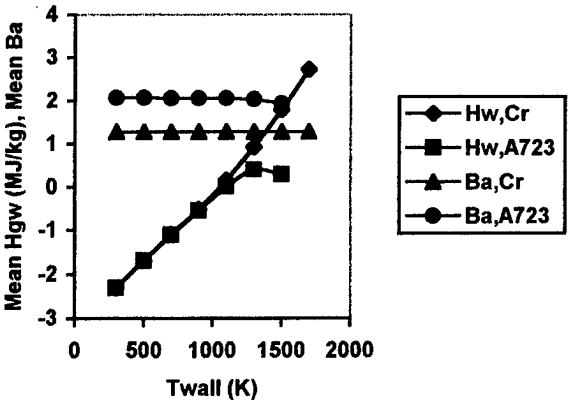

Figure 5 - M829E3 CCET G-W Thermochemistry.

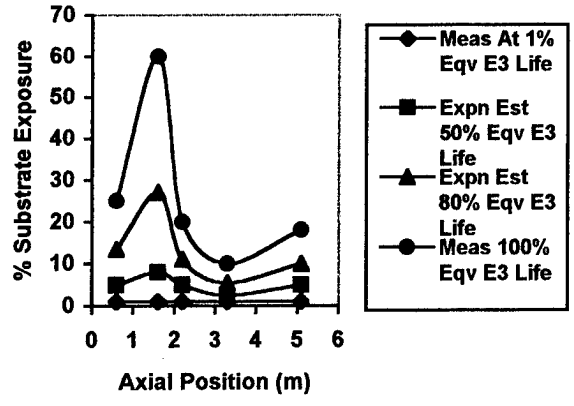

Figure 6 – M829E3 M256 Substrate Exposure.

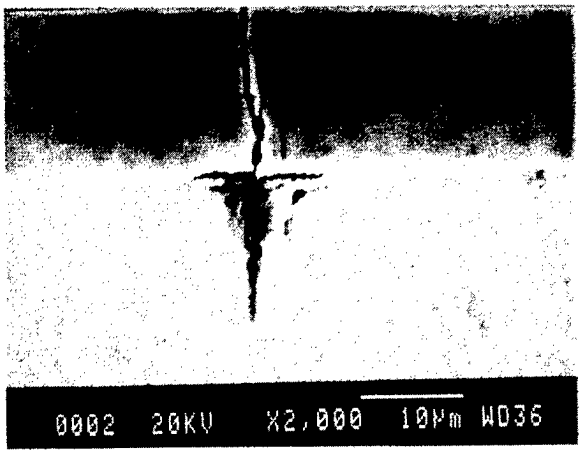

Figure 7 – M829E3 Peak Enabling Erosion Step.

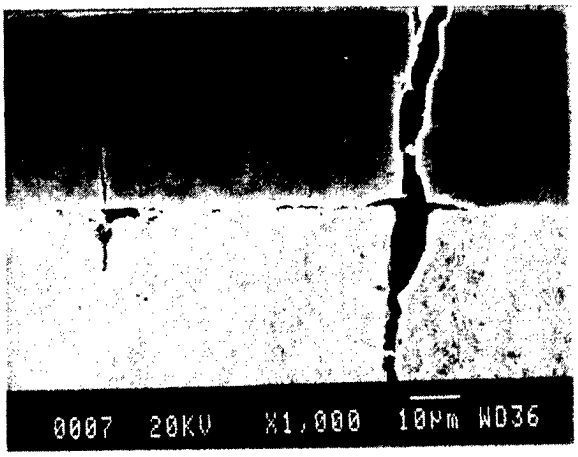

Figure 8 – M829E3 Peak Accelerating Erosion Step.

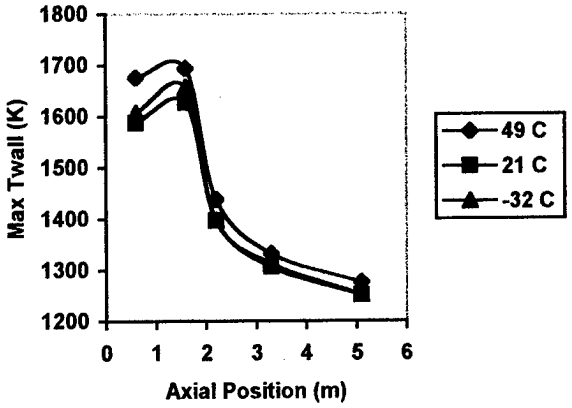

Figure 9 - M829E3 MACE HC Cr Surface Temp.

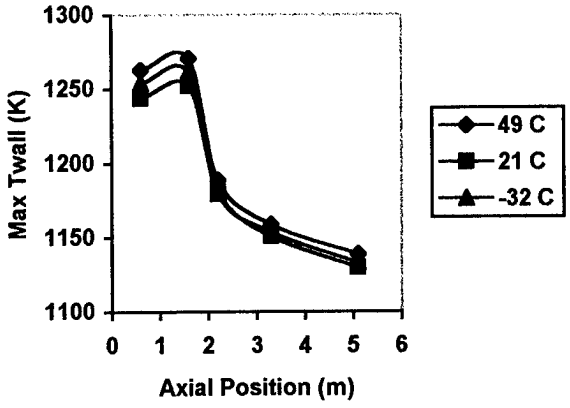

Figure 10-M829E3 MACE A723 Interface Temp.

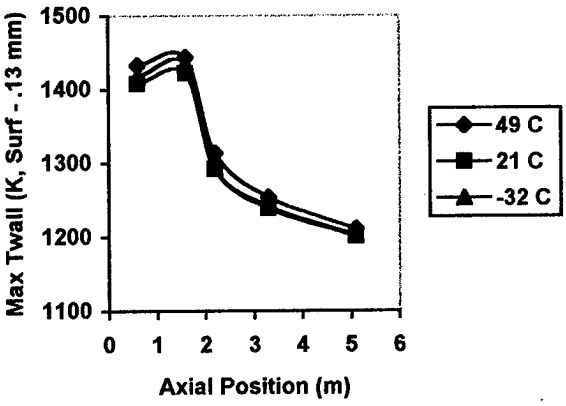

Figure 11 - M829E3 MACE A723 Surface Temp.

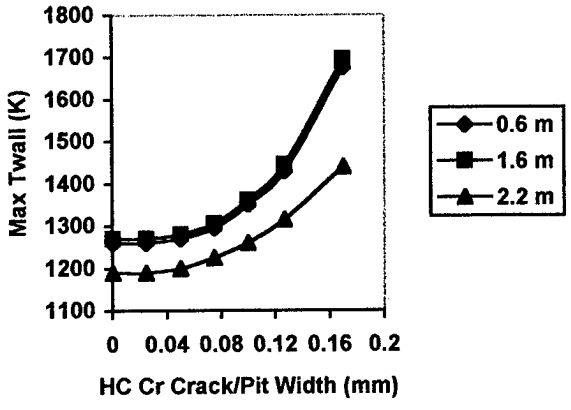

Fig. 12 - M829E3 Exposed Interface Temp.

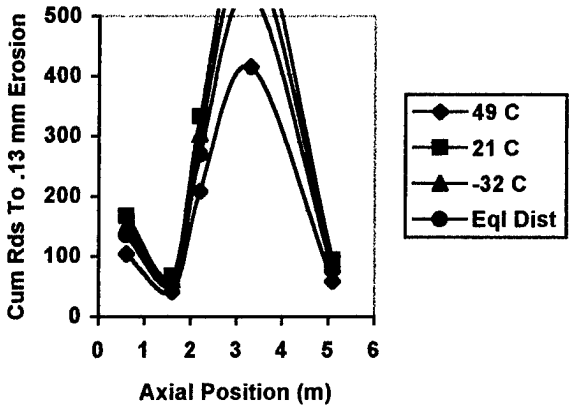

Figure 13 - M829E3 Erosion Onset.

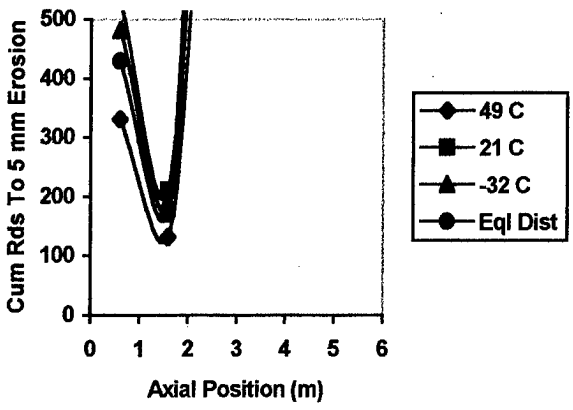

Figure 14- M829E3 Erosion Condemnation.

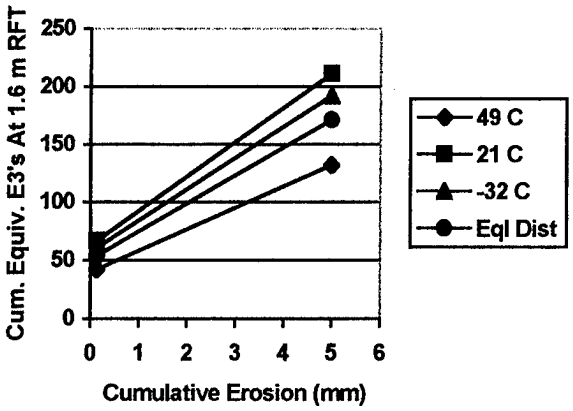

Figure 15 - M829E3 Erosion Summary.

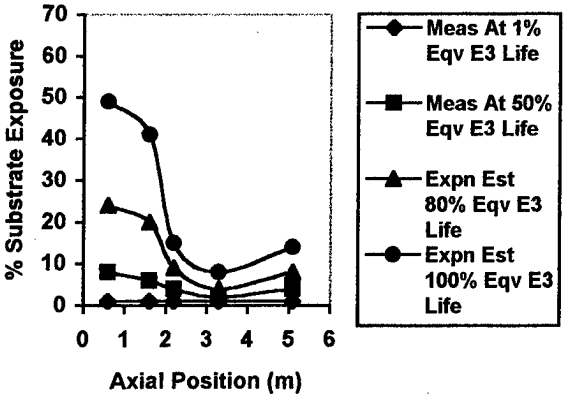

Fig. 16- E3/HEAT M256 Substrate Exposure.

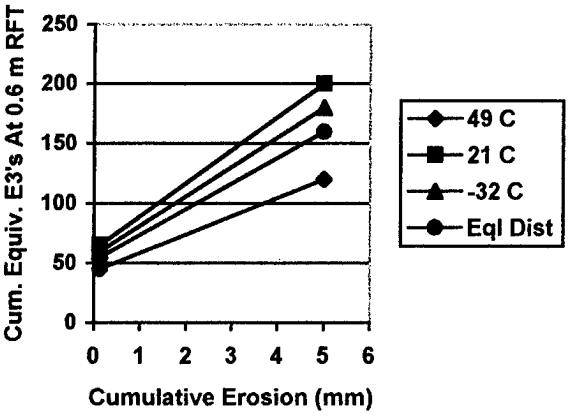

Fig. 17 - M829E3/HEAT Erosion Summary.